

## Classical Majorana-like zero modes in an acoustic Kitaev chain

An-Yang Guan,<sup>\*</sup> Zhang-Zhao Yang<sup>✉,\*</sup>, Wen-Jie Yang<sup>✉,\*</sup>, Xin Li, Xin-Ye Zou<sup>✉,†</sup> and Jian-Chun Cheng<sup>✉</sup>

Key Laboratory of Modern Acoustics, MOE, Institute of Acoustics, Department of Physics,  
Collaborative Innovation Center of Advanced Microstructures, Nanjing University, Nanjing 210093, People's Republic of China



(Received 13 May 2022; revised 28 March 2023; accepted 30 March 2023; published 10 April 2023)

The one-dimensional Kitaev chain, being one of the most significant superconductor models that support Majorana fermions, has been considered as a highly probable method to host nonlocal qubits for topological quantum computation. Here we theoretically introduce the concept into the classical-wave systems and report the first experimental prototype of the acoustic Kitaev chain. We rigorously demonstrate the acoustic correspondence of the Kitaev chain and experimentally observe the classical unpaired Majorana-like zero mode in a well-designed acoustic spinless  $p$ -wave superconductor. In particular, clear physical evidence also demonstrates such exotic acoustic modes can be manipulated to a certain extent like a quasiparticle, which is directly identified by employing a Kitaev “keyboard.” These results are expected to open new avenues for novel applications of topological acoustics.

DOI: [10.1103/PhysRevB.107.134107](https://doi.org/10.1103/PhysRevB.107.134107)

### I. INTRODUCTION

The concept of topological insulators characterized by multiple topological phases has attracted extensively investigation [1–4]. Due to the ability of manipulating the special robust electronic states that against microscopic disorder and supporting lossless energy transportation [5], topological insulators, and topological superconductors in different classifications have been considered with significant potential for quantum technologies [6–8]. Remarkably, in the field of topological quantum computation, topological superconductors are predicted to hold considerable solution to find a class of non-Abelian anyons, namely the Majorana fermions, which may embed quantum information in a nonlocal and intrinsically decoherence-free fashion for the experimental synthesis of a quantum computer [9–11]. In 2001, Kitaev proposed the celebrated one-dimensional (1D) toy model of a spinless  $p$ -wave superconducting  $N$ -site chain that can support the unpaired end-Majorana zero modes degenerate at zero energy as the system being topologically nontrivial [12], which has inspired a series of research on realizing such the 1D superconducting wires in superfluids and superconductors [13–22], whereas it remains an ongoing challenge to synthesize a real chain due to the absence of hypothetical spinless fermions and the uncommonness of  $p$ -wave pairing.

On the other hand, the classical-wave systems as its flexibility and reconfigurability have long been considered as a prominent platform for engineering topological energy bands and observing novel quantum phenomena [23–30]. Recently, the quantum Hall effect [31], quantum spin Hall effect [32], and higher-order topology [33] have been directly demonstrated in mechanical [34–38], photonic [39–41], electrical circuits [42–44], and acoustic systems [45–47]. Critically,

although mechanical counterparts of the Kitaev chain have been studied in some works experimentally [48,49], whether an analog of the Kitaev chain with observable Majorana-like zero modes can be implemented in the classical-wave systems is still an open question.

In this article, the concept of spinless  $p$ -wave Kitaev chain is theoretically and experimentally introduced to acoustic system, and the created Majorana-like zero mode nature within the rigorous correspondence is revealed clearly. In contrast with atomic system, the Majorana-like zero modes in the conceived 1D acoustic wire does not require additional external fields for employing superconducting proximity effects and can be directly excited by sound stimuli. By judiciously designing a 1D wire network of the Kitaev chain based on resonance acoustic system, topological phase transition from the bulk spectrum along with the emergence of the unpaired Majorana zero modes can be observed exactly. Crucially, experiments are also conducted to not only verify the existence of such the exotic topological states but also demonstrate a “keyboard” property of the presented structure with individually tunable configuration to the chain that allows local control of the topology of each site and hence freely manipulate the analogous Majorana fermions while maintaining the bulk gap. Such the fascinating results are particularly meaningful in the classical-wave systems and may open up new avenues for helping the exploration of novel quantumlike materials in a macro scale.

### II. MAJORANA FERMIONS IN 1D KITAEV CHAIN

Let us focus our attention on the minimal Hamiltonian  $H$  describing the Kitaev toy model for a spinless  $p$ -wave superconducting  $N$ -site chain, which takes the form [12]

$$H = -\mu \sum_{n=1}^N c_n^\dagger c_n - \sum_{n=1}^{N-1} (t c_{n+1}^\dagger c_n + \Delta c_n c_{n+1} + \text{H.c.}), \quad (1)$$

<sup>\*</sup>These authors have contributed equally to this work.

<sup>†</sup>xyzou@nju.edu.cn

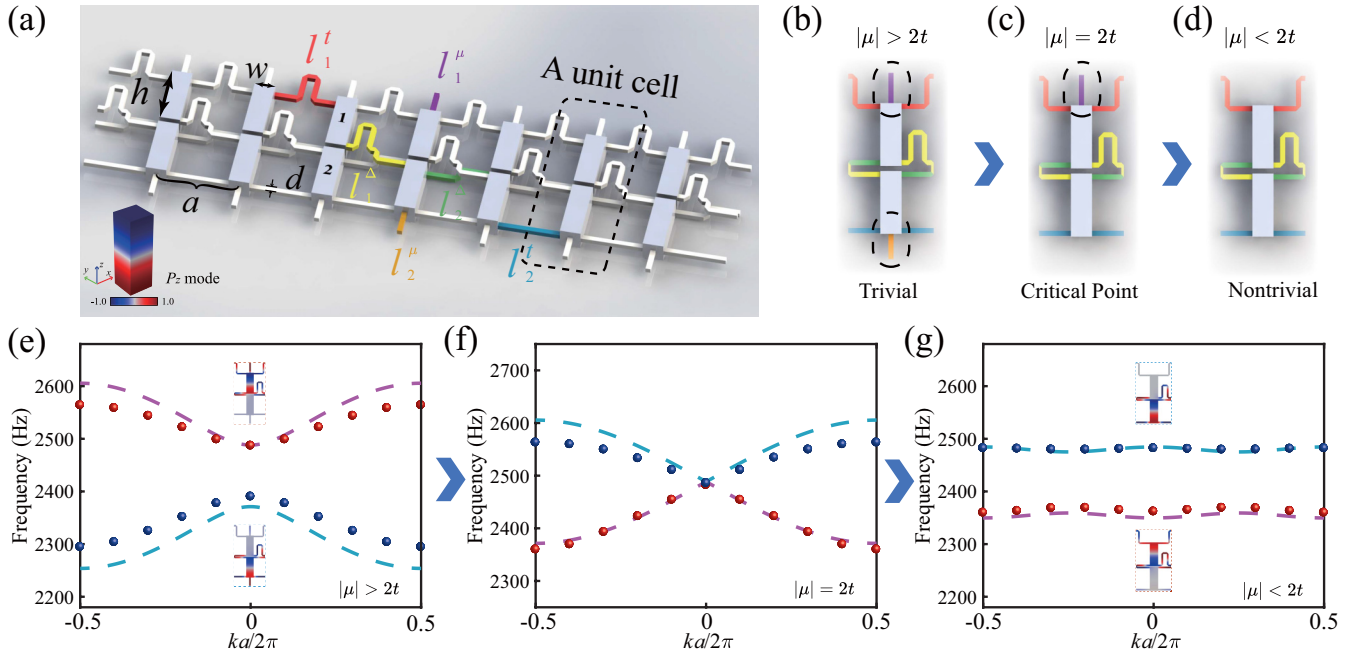


FIG. 1. (a) Schematic of the acoustic Kitaev chain. Insets: Defined  $P_z$  mode propagating in the structure. [(b)–(d)] Topological phase transition process in the unit cell with (b)  $l_1^\mu = 4.1$  cm and  $l_2^\mu = 3$  cm with  $\mu = -738$ ; (c)  $l_1^\mu = 4.1$  cm and  $l_2^\mu = 0$  cm with  $\mu = -368$ ; and (d)  $l_1^\mu = l_2^\mu = 0$  cm with  $\mu = 0$ , respectively. [(e)–(g)] Compare of the theoretical (dashed lines) and simulated (dots) energy band structures that correspond to (b)–(d), respectively. Insets: Sound pressure at  $k = 0$  distributes in the form of  $[1, 0]^T$  and  $[0, 1]^T$ , respectively, and the inversion indicates topological phase transition.

where  $t > 0$ ,  $\mu$ , and  $\Delta$  denotes the nearest-neighbor hopping strength, chemical potential, and  $p$ -wave pairing amplitude, respectively.  $c_n$  is the spinless fermion operator at  $n$ th site. Once imposing periodic boundary condition, the Bogoliubov–de Gennes Hamiltonian in the momentum space can then be written as

$$H = \frac{1}{2} \sum_k C_k^\dagger \mathcal{H}(k) C_k, \quad (2)$$

where  $C_k^\dagger = [c_k^\dagger, c_{-k}]$  and  $\mathcal{H}(k) = (-2t \cos k - \mu)\tau_z + 2\Delta \sin k \tau_y$ , where  $\tau$  is the Pauli matrix. Further, by diagonalizing  $\mathcal{H}(k)$ , one immediately obtain the bulk energy levels  $E(k) = \pm \sqrt{(2t \cos k + \mu)^2 + 4\Delta^2 \sin^2 k}$ . Accordingly, a bulk gap closing at  $k = 0$  happens when  $|\mu| = 2t$ , which exactly indicates the critical point of topological phase transition.

Additionally, although it is well known that the condensed matter systems are made of electrons which always correspond to paired Majorana fermions, it turns out that the unpaired Majoranas, which is key in the Kitaev chain, can be realized by engineering the Hamiltonian in some special ways. To understand the topological phase transition along with the emergence of the unpaired Majoranas in the chain, we now replace the spinless fermion  $c_n$  with the Majorana operator  $\gamma_{n,a}$  and  $\gamma_{n,b}$  (where  $\gamma_{n,\alpha} = \gamma_{n,\alpha}^\dagger$ ) as  $c_n = (\gamma_{n,a} - i\gamma_{n,b})/2$ , and Eq. (1) then can be rewritten as

$$H = \frac{i}{2} \left\{ \sum_{n=1}^{N-1} [(-\Delta - t)\gamma_{n,b}\gamma_{n+1,a} + (-\Delta + t)\gamma_{n+1,b}\gamma_{n,a}] + \mu \sum_{n=1}^N \gamma_{n,a}\gamma_{n,b} \right\}. \quad (3)$$

Further, two limiting cases are cautiously considered. In the first case we set  $\Delta = t = 0$  with  $\mu \neq 0$ , and  $H$  is then reduced to  $H = (i/2)\mu \sum_{n=1}^N \gamma_{n,a}\gamma_{n,b}$ , which indicates the Majorana modes  $\gamma_{n,a}$  and  $\gamma_{n,b}$  always pair in the same site and corresponds to a trivial phase. Crucially, in the second limiting case with  $\Delta = t$  and  $\mu = 0$ ,  $H = it \sum_{n=1}^{N-1} \gamma_{n,b}\gamma_{n+1,a}$  indicates the Majoranas are paired up from the adjacent sites, which naturally leaves  $\gamma_{1,a}$  and  $\gamma_{N,b}$  being unpaired and act as the end-Majorana modes degenerate at zero energy due to particle-hole symmetry. Meanwhile, the pair of wave functions  $[1, 0]^T$  and  $[0, 1]^T$  is inverted at high symmetry point also indicates the topological phase transition. As a result,  $|\mu| < 2t$  represents the nontrivial superconducting states with a partially filled band pairs, while  $|\mu| > 2t$  corresponds to the trivial topology without Majoranas emerging.

### III. ACOUSTIC KITAEV CHAIN AND CLASSICAL MAJORANA-LIKE ZERO MODES

We now focus on the acoustic correspondence of the Kitaev chain discussed above, and the 1D wire structure with the lattice constant  $a$  is depicted in Fig. 1(a). Here each unit cell consists of two individual cuboid acoustic cavities with its length and width as  $w$  and the height  $h$ , respectively. The unit cells are complicatedly connected by four bent tubes (respectively marked in red, yellow, blue, and green in Fig. 1(a)) with identical side-length  $d$  and effective lengths  $l_1^\mu$ ,  $l_2^\mu$ ,  $l_1^\Delta$ , and  $l_2^\Delta$ , respectively. In addition, two extra tubes (respectively marked in purple and orange) with tunable lengths  $l_1^\mu$  and  $l_2^\mu$  are connected with the two cavities in each unit cell, respectively. The sound speed and density of air are  $c_0$  and  $\rho_0$ , respectively,

and the outermost tubes are all closed with acoustic hard boundaries.

For synthesizing the analogous Majorana fermions, we now consider the sound wave propagating within the system in a  $P_z$  mode [Fig. 1(a)], which corresponds to the dipolar standing wave with frequency  $\omega_0$ . Accordingly, the normalized field distribution of acoustic velocity potential in  $j$ th ( $j = 1, 2$ ) cavity of each unit cell can be written as  $\psi_j(\vec{r}) = \sqrt{2/(w^2h)}\sin(\pi r_z/h)$ , where  $r_z$  is the component of  $\vec{r}$  in the  $z$  direction. Further, by defining the parameters  $\xi = [\xi_1, \xi_2]^T$ , where  $\xi_j = p_j(\vec{r})/\psi_j(\vec{r})$  and  $p_j(\vec{r})$  is the corresponding sound pressure, the distribution of the sound field in the representation of  $\xi$  with propagating frequency  $\omega$  then satisfies

$$\omega\xi = [\mathcal{H}_0 + \mathcal{H}_a(k)]\xi, \quad (4)$$

where

$$\mathcal{H}_0 = \begin{pmatrix} \omega_0 + \epsilon_1 & 0 \\ 0 & \omega_0 + \epsilon_2 \end{pmatrix},$$

$$\mathcal{H}_a(k) = \begin{bmatrix} \mu_1 + 2t_1 \cos(ka) & \Delta_1 e^{ika} + \Delta_2 e^{-ika} \\ \Delta_1 e^{-ika} + \Delta_2 e^{ika} & \mu_2 + 2t_2 \cos(ka) \end{bmatrix}, \quad (5)$$

where  $\epsilon_1 = (c_0 d^2 |\bar{\psi}|^2 / 2) [2 \cot(\omega_0 l_1^t / c_0) + \cot(\omega_0 l_1^\Delta / c_0) + \cot(\omega_0 l_2^\Delta / c_0)]$  represents a total perturbation induced by the connected tubes on the corresponding cavity and  $\epsilon_2$  takes the same form with opposite subscripts. Crucially, the key correspondences are clearly determined as  $t_j = -(c_0 d^2 |\bar{\psi}|^2 / 2) \csc(\omega_0 l_j^t / c_0)$ ,  $\Delta_j = -(c_0 d^2 |\bar{\psi}|^2 / 2) \csc(\omega_0 l_j^\Delta / c_0)$ , and  $\mu_j = i(\rho_0 c_0^2 d^2) / (w^2 h Z_j^\mu)$ , respectively, where  $|\bar{\psi}|$  indicates the average of  $\psi(\vec{r})$  over the end of the tubes and  $Z_j^\mu = -i\rho_0 c_0 \cot(\omega_0 l_j^\mu / c_0)$  represents the impedance of the extra tube (see Sec. I in the Supplemental Material [50]). It is worth noting that all the parameters are naturally decoupled, the amplitude as well as sign therefore can be manipulated independently. Further, once setting  $l_1^t = l_1^\Delta + h$  and  $l_2^\Delta = l_2^t + h$ , we obtain  $\epsilon_1 = \epsilon_2$ ,  $t_1 = -t_2$ , and  $\Delta_1 = -\Delta_2$  and immediately find that  $\mathcal{H}_a(k)$  is rigorously equivalent to  $\mathcal{H}(k)$  in Eq. (2), while  $\mathcal{H}_0$  only contributes to a spectra shift in practice. As a result, the Kitaev chain can finally be implemented in acoustic system.

According to the discussion above, we now set  $w = 2.5$  cm,  $h = 7.5$  cm,  $d = 0.5$  cm,  $l_1^t = 18.25$  cm,  $l_2^t = 10.5$  cm,  $l_1^\Delta = 18.95$  cm, and  $l_2^\Delta = 11.2$  cm (therefore  $t = 184$  and  $\Delta = 180$ , respectively) in the following and exhibit the topological phase transition in the acoustic Kitaev chain by merely controlling  $l^\mu$ . Figures 1(b)–1(d) depict the process in the unit cell where  $|\mu| < 2t$ ,  $|\mu| = 2t$  and  $|\mu| > 2t$ , respectively, and the corresponding theoretical and numerical energy band structures are presented in Figs. 1(e)–1(g), respectively, which serves a good evidence of topological phase transition in the system (see Sec. II in the Supplemental Material [50]). In particular, as the key identified topological feature in the system, a pair of unpaired Majorana-like zero modes is predicted to emerge at the ends of the Kitaev chain. Pictorial representations of the Kitaev chain in the two limiting cases are sketched in Figs. 2(a) and 2(b), respectively, and the energy spectra of the acoustic correspondence spanning seven sites are presented in Figs. 2(c) and 2(d), respectively. It is clear to see that,

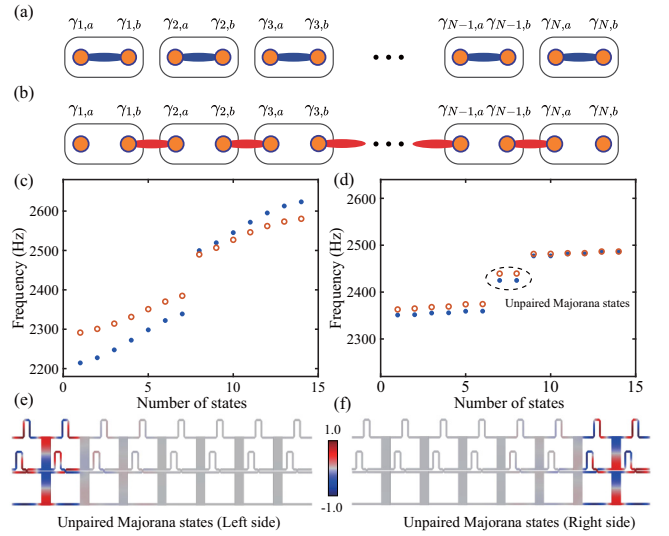


FIG. 2. [(a) and (b)] Pictorial representations of the Kitaev chain in the limiting cases  $\Delta = t = 0$ ,  $\mu \neq 0$  and  $\Delta = t \neq 0$ ,  $\mu = 0$ , respectively. [(c) and (d)] Eigenfrequency spectra of the finite acoustic chain in trivial and nontrivial phase, respectively. Blue dots and red circles represent theoretical and numerical results, respectively. [(e) and (f)] Field distributions of sound pressure of the unpaired Majorana-like zero modes at the ends of the acoustic Kitaev chain, respectively.

in contrast to a complete bulk gap when topologically trivial, two degenerate Majorana zero modes are exactly pinned at the frequency  $\omega_0 + \epsilon$  in the nontrivial phase. Crucially, the sound pressure field distributions of such the exotic modes exhibited in Figs. 2(e) and 2(f) demonstrate they are unpaired. In the following, experiments are performed in detail.

#### IV. EXPERIMENTAL REALIZATION OF A “KEYBOARD” OF THE KITAEV CHAIN

First, we consider the gap closing condition when  $|\mu| = 2t$ . After a linear expansion, the Hamiltonian  $\mathcal{H}(k)$  takes the form as

$$\mathcal{H}(k) = m\tau_z + 2\Delta k\tau_y, \quad (6)$$

where  $m = -\mu - 2t$  is the mass term. As a result,  $m = 0$  represents a critical point and the opposite sign of  $m$  therefore indicates different topological phase, which reminds us that the Majorana-like zero modes can emerge as domain-wall states between two domains with different topology. As illustrated in Fig. 3(a), we construct an acoustic sample with a domain wall between six trivial ( $m > 0$ ) and six nontrivial ( $m < 0$ ) unit cells. To identify the Majorana zero mode, each site cavity is perforated with a hole (sealed when not in measurement), and a broadband acoustic stimuli is placed outside the sample near the domain wall. Figure 3(b) shows the measured intensity spectra, and it is clear to see a spectrally isolated peak at around 2430 Hz, which exactly corresponds to the Majorana zero mode predicted in Fig. 2(b). Meanwhile, the measured spatial distribution of the Majorana-like zero mode is presented in Fig. 3(c), which exhibits the locality of

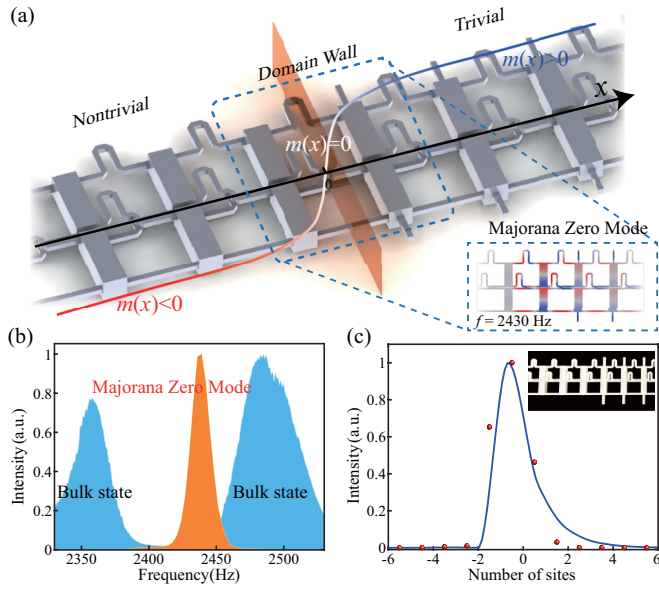


FIG. 3. (a) Schematic of the domain-wall between topological trivial and nontrivial domains. Insets: Acoustic domain-wall Majorana-like zero mode. (b) Experimentally measured bulk (cyan) and domain-wall (orange) spectra. (c) Comparison of measured (red dots) and numerical (blue line) spatial distribution of the existing domain-wall state. Inset: Photograph of the 3D printed acoustic Kitaev chain.

Majorana wave function (see Sec. III in the Supplemental Material [50]). Accordingly, such the experimental results confirm the classical Majorana-like zero modes existing in the acoustic Kitaev chain.

Finally, in the theoretical model, as long as the chemical potential is regulated, the Majorana fermions can be manipulated, which brings inspiration to the acoustic system. We perform experiments of the Kitaev “keyboard” to verify the quasiparticle character of the acoustic Majorana-like zero modes [10]. Due to the decoupled  $\mu$  and  $t$  in the presented structure, we now define a gate where a topological phase represents “ON” while the trivial phase “OFF” as depicted in Fig. 4(a), and the gate can be easily switched by tuning  $l^\mu$  [Fig. 4(b)]. Correspondingly, the given gates are controlled locally, which allows analogous Majoranas to be created, transported, and fused freely. Figures 4(c) outlines the setup of a Kitaev “keyboard” spanning 12 sites, which corresponds to three independent experiments, and the measured spatial intensity distributions are presented in Figs. 4(d)–4(f), respectively. Accordingly, an unpaired Majorana-like zero mode is driven from site 2 to site 6 in the transport process [Fig. 4(d)], and the acoustic modes can be either fused into a single finite-energy mode [site 5 and site 8 in Fig. 4(e)] or created [site 5 and site 8 in Fig. 4(f)] by controlling the gates (see Sec. IV in the Supplemental Material [50]). The measured results directly demonstrate the acoustic Majorana-like zero modes may act as quasiparticles. In addition, compared with some existing models such as acoustic Su-Schrieffer-Heeger model, we only need to regulate the length of the additional tubes in our model, and we can easily implement a variety of

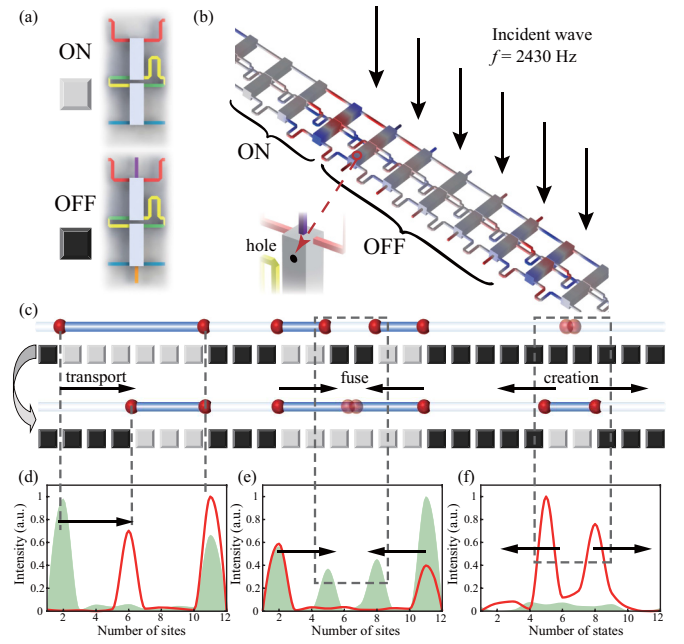


FIG. 4. (a) Schematic of the acoustic gates. (b) Experimental setup of the acoustic Kitaev keyboard. (c) Pictorial representations of the transport, fuse, and creation process of the analogous Majorana fermions. [(d)–(f)] Experimentally measured spatial intensity distributions of the acoustic Majorana zero modes before (green area) and after (red line) specific operations corresponding to (c), respectively.

functions in a single sample. This advantage comes from the Kitaev chain that only needs to regulate chemical potential to manipulate Majorana fermions.

## V. CONCLUSIONS

To conclude, we have theoretically extended the 1D Kitaev chain into acoustic system for sound waves and experimentally observed the classical Majorana-like zero modes as well as verified its particular characters. By precisely proposing the correspondence of the 1D Kitaev chain in resonance acoustic system, the unpaired Majorana-like zero modes can be directly observed. In particular, clear evidence manifests that by freely controlling the gates, such the exotic acoustic modes can be created, transported, and fused, which act like quasiparticles. As a result, this work constitutes the first classical-wave demonstration of analogous Majorana-like fermions based on a stringent acoustic Kitaev chain. Beyond its fundamental significance, this framework is expected to enrich the inherent physics and broaden roads for the design and applications of future topological metamaterials.

## ACKNOWLEDGMENTS

This work was supported by the National Key R&D Program of China (Grant No. 2017YFA0303700), National Natural Science Foundation of China (Grants No. 11634006, No. 11934009, 12274219, and 12074184), and the Natural Science Foundation of Jiangsu Province (Grant No. BK20191245).

- [1] M. Z. Hasan and C. L. Kane, Colloquium: Topological insulators, *Rev. Mod. Phys.* **82**, 3045 (2010).
- [2] J. E. Moore, The birth of topological insulators, *Nature (London)* **464**, 194 (2010).
- [3] X.-L. Qi and S.-C. Zhang, Topological insulators and superconductors, *Rev. Mod. Phys.* **83**, 1057 (2011).
- [4] C.-K. Chiu, J. C. Y. Teo, A. P. Schnyder, and S. Ryu, Classification of topological quantum matter with symmetries, *Rev. Mod. Phys.* **88**, 035005 (2016).
- [5] Y. Ando and L. Fu, Topological crystalline insulators and topological superconductors: From concepts to materials, *Annu. Rev. Condens. Matter Phys.* **6**, 361 (2015).
- [6] C. Kallin and J. Berlinsky, Chiral superconductors, *Rep. Prog. Phys.* **79**, 054502 (2016).
- [7] M. Sato and Y. Ando, Topological superconductors: A review, *Rep. Prog. Phys.* **80**, 076501 (2017).
- [8] K. Kawabata, Y. Ashida, H. Katsura, and M. Ueda, Parity-time-symmetric topological superconductor, *Phys. Rev. B* **98**, 085116 (2018).
- [9] C. Nayak, S. H. Simon, A. Stern, M. Freedman, and S. Das Sarma, Non-Abelian anyons and topological quantum computation, *Rev. Mod. Phys.* **80**, 1083 (2008).
- [10] J. Alicea, Y. Oreg, G. Refael, F. Von Oppen, and M. P. A. Fisher, Non-Abelian statistics and topological quantum information processing in 1d wire networks, *Nat. Phys.* **7**, 412 (2011).
- [11] J. D. Sau, D. J. Clarke, and S. Tewari, Controlling non-Abelian statistics of Majorana fermions in semiconductor nanowires, *Phys. Rev. B* **84**, 094505 (2011).
- [12] A. Y. Kitaev, Unpaired Majorana fermions in quantum wires, *Phys. Usp.* **44**, 131 (2001).
- [13] M. Freedman, C. Nayak, and K. Walker, Towards universal topological quantum computation in the  $\nu = 5/2$  fractional quantum Hall state, *Phys. Rev. B* **73**, 245307 (2006).
- [14] R. M. Lutchyn, J. D. Sau, and S. Das Sarma, Majorana Fermions and a Topological Phase Transition in Semiconductor-Superconductor Heterostructures, *Phys. Rev. Lett.* **105**, 077001 (2010).
- [15] Y. Oreg, G. Refael, and F. von Oppen, Helical Liquids and Majorana Bound States in Quantum Wires, *Phys. Rev. Lett.* **105**, 177002 (2010).
- [16] J. D. Sau, R. M. Lutchyn, S. Tewari, and S. Das Sarma, Generic New Platform for Topological Quantum Computation Using Semiconductor Heterostructures, *Phys. Rev. Lett.* **104**, 040502 (2010).
- [17] L. Fidkowski and A. Kitaev, Topological phases of fermions in one dimension, *Phys. Rev. B* **83**, 075103 (2011).
- [18] J. Alicea, New directions in the pursuit of Majorana fermions in solid state systems, *Rep. Prog. Phys.* **75**, 076501 (2012).
- [19] J. D. Sau and S. D. Sarma, Realizing a robust practical Majorana chain in a quantum-dot-superconductor linear array, *Nat. Commun.* **3**, 964 (2012).
- [20] M. Greiter, V. Schnells, and R. Thomale, The 1d Ising model and the topological phase of the Kitaev chain, *Ann. Phys.* **351**, 1026 (2014).
- [21] Q. Wang, C.-C. Liu, Y.-M. Lu, and F. Zhang, High-Temperature Majorana Corner States, *Phys. Rev. Lett.* **121**, 186801 (2018).
- [22] C. Zeng, T. D. Stanescu, C. Zhang, V. W. Scarola, and S. Tewari, Majorana Corner Modes with Solitons in an Attractive Hubbard-Hofstadter Model of Cold Atom Optical Lattices, *Phys. Rev. Lett.* **123**, 060402 (2019).
- [23] Z. Yang, F. Gao, X. Shi, X. Lin, Z. Gao, Y. Chong, and B. Zhang, Topological Acoustics, *Phys. Rev. Lett.* **114**, 114301 (2015).
- [24] X. Ni, M. Weiner, A. Alù, and A. B. Khanikaev, Observation of higher-order topological acoustic states protected by generalized chiral symmetry, *Nat. Mater.* **18**, 113 (2019).
- [25] C. W. Peterson, W. A. Benalcazar, T. L. Hughes, and G. Bahl, A quantized microwave quadrupole insulator with topologically protected corner states, *Nature (London)* **555**, 346 (2018).
- [26] P. Gao, D. Torrent, F. Cervera, P. San-Jose, J. Sánchez-Dehesa, and J. Christensen, Majorana-Like Zero Modes in Kekulé Distorted Sonic Lattices, *Phys. Rev. Lett.* **123**, 196601 (2019).
- [27] J. Noh, T. Schuster, T. Iadecola, S. Huang, M. Wang, K. P. Chen, C. Chamon, and M. C. Rechtsman, Braiding photonic topological zero modes, *Nat. Phys.* **16**, 989 (2020).
- [28] Z.-G. Chen, R.-Y. Zhang, C. T. Chan, and G. Ma, Classical non-Abelian braiding of acoustic modes, *Nat. Phys.* **18**, 179 (2021).
- [29] X. Huang, J. Lu, Z. Yan, M. Yan, W. Deng, G. Chen, and Z. Liu, Acoustic higher-order topology derived from first-order with built-in Zeeman-like fields, *Sci. Bull.* **67**, 488 (2021).
- [30] B. Jiang, A. Bouhon, Z.-K. Lin, X. Zhou, B. Hou, F. Li, R.-J. Slager, and J.-H. Jiang, Experimental observation of non-Abelian topological acoustic semimetals and their phase transitions, *Nat. Phys.* **17**, 1239 (2021).
- [31] F. D. M. Haldane, Model for a Quantum Hall Effect Without Landau Levels: Condensed-Matter Realization of the “Parity Anomaly”, *Phys. Rev. Lett.* **61**, 2015 (1988).
- [32] C. L. Kane and E. J. Mele, Quantum Spin Hall Effect in Graphene, *Phys. Rev. Lett.* **95**, 226801 (2005).
- [33] W. A. Benalcazar, T. Li, and T. L. Hughes, Quantization of fractional corner charge in  $cn$ -symmetric higher-order topological crystalline insulators, *Phys. Rev. B* **99**, 245151 (2019).
- [34] M. Miniaci, R. K. Pal, B. Morvan, and M. Ruzzene, Experimental Observation of Topologically Protected Helical Edge Modes in Patterned Elastic Plates, *Phys. Rev. X* **8**, 031074 (2018).
- [35] R. Chaunsali, C.-W. Chen, and J. Yang, Experimental demonstration of topological waveguiding in elastic plates with local resonators, *New J. Phys.* **20**, 113036 (2018).
- [36] M. Serra-Garcia, V. Peri, R. Süsstrunk, O. R. Bilal, T. Larsen, L. G. Villanueva, and S. D. Huber, Observation of a phononic quadrupole topological insulator, *Nature (London)* **555**, 342 (2018).
- [37] Q. Zhang, Y. Chen, K. Zhang, and G. Hu, Dirac degeneracy and elastic topological valley modes induced by local resonant states, *Phys. Rev. B* **101**, 014101 (2020).
- [38] H. Wakao, T. Yoshida, H. Araki, T. Mizoguchi, and Y. Hatsugai, Higher-order topological phases in a spring-mass model on a breathing kagome lattice, *Phys. Rev. B* **101**, 094107 (2020).
- [39] J. Noh, W. A. Benalcazar, S. Huang, M. J. Collins, K. P. Chen, T. L. Hughes, and M. C. Rechtsman, Topological protection of photonic mid-gap defect modes, *Nat. Photon.* **12**, 408 (2018).
- [40] L. He, Z. Addison, E. J. Mele, and B. Zhen, Quadrupole topological photonic crystals, *Nat. Commun.* **11**, 3119 (2020).
- [41] B. Xie, G. Su, H.-F. Wang, F. Liu, L. Hu, S.-Y. Yu, P. Zhan, M.-H. Lu, Z. Wang, and Y.-F. Chen, Higher-order quantum spin Hall effect in a photonic crystal, *Nat. Commun.* **11**, 3768 (2020).
- [42] S. Imhof, C. Berger, F. Bayer, J. Brehm, L. W. Molenkamp, T. Kiessling, F. Schindler, C. H. Lee, M. Greiter, T. Neupert,

- and R. Thomale, Topoelectrical-circuit realization of topological corner modes, *Nat. Phys.* **14**, 925 (2018).
- [43] X. Ni, Z. Xiao, A. B. Khanikaev, and A. Alù, Robust Multiplexing with Topoelectrical Higher-Order Chern Insulators, *Phys. Rev. Appl.* **13**, 064031 (2020).
- [44] W. Zhang, D. Zou, Q. Pei, W. He, J. Bao, H. Sun, and X. Zhang, Experimental Observation of Higher-Order Topological Anderson Insulators, *Phys. Rev. Lett.* **126**, 146802 (2021).
- [45] C. He, X. Ni, H. Ge, X.-C. Sun, Y.-B. Chen, M.-H. Lu, X.-P. Liu, and Y.-F. Chen, Acoustic topological insulator and robust one-way sound transport, *Nat. Phys.* **12**, 1124 (2016).
- [46] Y. Qi, C. Qiu, M. Xiao, H. He, M. Ke, and Z. Liu, Acoustic Realization of Quadrupole Topological Insulators, *Phys. Rev. Lett.* **124**, 206601 (2020).
- [47] B. Hu, Z. Zhang, H. Zhang, L. Zheng, W. Xiong, Z. Yue, X. Wang, J. Xu, Y. Cheng, X. Liu, and J. Christensen, Non-hermitian topological whispering gallery, *Nature (London)* **597**, 655 (2021).
- [48] E. Prodan, K. Dobiszewski, A. Kanwal, J. Palmieri, and C. Prodan, Dynamical Majorana edge modes in a broad class of topological mechanical systems, *Nat. Commun.* **8**, 14587 (2017).
- [49] F. Allein, R. Chaunsali, A. Anastasiadis, I. Frankel, N. Boechler, F. K. Diakonov, and G. Theocharis, Duality of topological edge states in a mechanical Kitaev chain, [arXiv:2203.10311](https://arxiv.org/abs/2203.10311).
- [50] See Supplemental Material at <http://link.aps.org/supplemental/10.1103/PhysRevB.107.134107> for more details on derivation of the acoustic correspondence of one-dimensional Kitaev chain, topological properties of the acoustic Kitaev chain, details of simulations and experiments, numerical results of the acoustic Kitaev and the particle-hole symmetry of acoustic system.